

Tracing cross-free polylines oriented by a N-symmetry direction field on triangulated surfaces

N. Ray*
INRIA

D. Sokolov†
Université de Lorraine

October 30, 2018

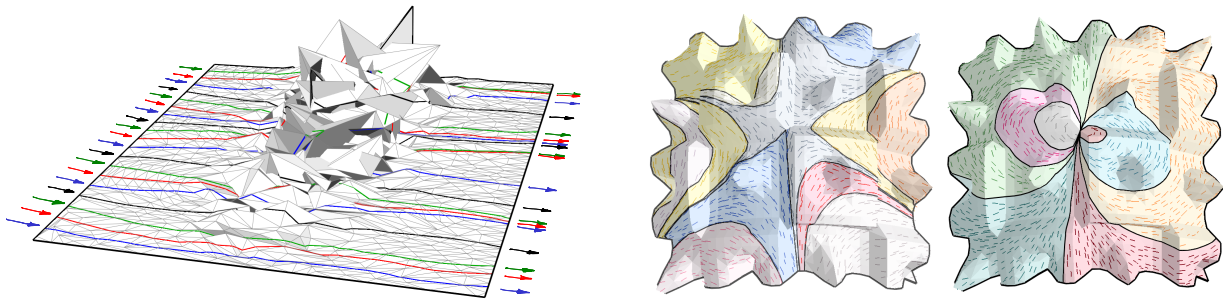


Figure 1: Our algorithm traces polylines on triangulated surfaces. Unlike streamline tracing algorithms, polylines produced by our technique cannot cross each others. It works even with highly perturbed surfaces (left) and supports any type of vector field singularities (right). This property is required to segment surfaces with chart boundaries aligned with a vector field (right).

Abstract

We propose an algorithm for tracing polylines on a triangle mesh such that: they are aligned with a N-symmetry direction field, and two such polylines cannot cross or merge. This property is fundamental for mesh segmentation and is very difficult to enforce with numerical integration of vector fields. We propose an alternative solution based on “stream-mesh”, a new combinatorial data structure that defines, for each point of a triangle edge, where the corresponding polyline leaves the triangle. It makes it possible to trace polylines by iteratively crossing trian-

gles. Vector field singularities and polyline/vertex crossing are characterized and consistently handled. The polylines inherits the cross-free property of the stream-mesh, except inside triangles where avoiding local overlaps would require higher order polycurves.

1 Introduction

Segmentation of triangulated surfaces that aligns chart boundaries with a vector field (or, more generally, a direction field) often exhibits useful properties for computer graphics applications. For instance, alignment with the main curvature directions allows for quad dominant remeshing [ACSD⁺03], following the gradient of a scalar field allows to compute

*e-mail: ray@loria.fr

†e-mail: sokolovd@loria.fr

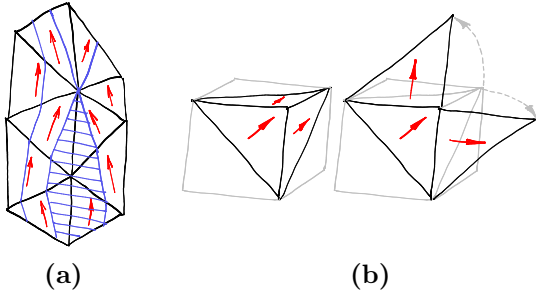


Figure 2: **(a)** all streamlines from the dashed area merge on an edge, and split on a vertex. **(b)** constant per triangle tangent vector fields have direction discontinuities along edges due to vertex angle defect.

pure quad decomposition using Morse-Smale complexes [DBG⁺06, SZ12], and streamlines of a cross field can decompose a mesh into quad shaped domains [KLF13].

The simplest solution to trace such polylines is to define a constant per triangle vector field. However, in this representation, streamlines will have merging, splittings and crossings, as illustrated in Figure 2(a) and further detailed in [SZ12]. As explained in Section 2, only Zhang *et al*'s vector field representation [ZMT06] allows to completely avoid these issues, but computing accurate enough streamlines is still very difficult.

The continuous counter part of our problem would be to trace streamlines of a vector field tangent to a smooth surface. As continuous streamlines do not cross, an accurate enough numerical field integration will share this property. The representation of Zhang *et al* provides an equivalent smooth problem without having to refine the field and the surface. We can therefore characterize the integration accuracy only by the step length of the order four Runge-Kutta field integration algorithm. In practice, the field is derived from the surface geometry, making it common to have streamlines very close to each other (local symmetries, almost aligned singularities, etc.). We observed (Figure 3) that with a integration step length higher than equals to 1/100 times the average edge length, most models have at least one streamline crossing. From a practical point of view, an ac-

curacy that would prevents most conflicts ($\approx 1/1000$ times the average edge length) is more than 100 times slower than our algorithm. Moreover, it would be very difficult to refine the integration because: tracing a streamline is a basic operation of the segmentation process and removing a crossing requires to refine both streamlines, and higher accuracy may produce new crossings.

Our solution is much faster than numerical field integration (crossing a triangle takes approximately the time to perform 10 RK4 steps), and allows to prevent crossings without tuning any “accuracy” parameters. Those benefits come at the expense of the fitting quality with the input field. For mesh segmentation, where the input field only give a coarse approximation of the desired edge direction [RLL⁺06, MPKZ10, KLF13], it is more important to have a guaranty that streamlines will not cross than a better fitting with the input field.

An overview of our method is presented in Algorithm 1 and illustrated in Figure 4. For each crossed triangle we construct on the fly a stream-mesh structure which is essentially the original triangle split in a way that each stream-halfedge can be flagged as input/output/tangent. Each vertex of the polyline is defined by its underlying mesh halfedge e , and its barycentric coordinate c (and $1 - c$) on this halfedge. A similar representation e_{sm}, c_{sm} is used for crossing the stream-mesh. A streamline finish either when the halfedge has no associated facet (mesh boundary), or when $c \in [1 \dots 2]$ instead of being in $[0 \dots 1]$ to denote an output on a singular vertex e.g. a sink of the vector field.

Limitation Having a single polyline segment inside each triangle may produce degenerated geometries: local (limited to a single edge) overlaps and regions of triangle that are not covered by any polyline (inset figure of section 4).

Previous Works

To the best of our knowledge, no prior work directly addresses our problem. However, it is interesting to consider solutions developed for 2D streamline tracing, to notice similar issues occurring for tracing other types of curves on surfaces, and to give an

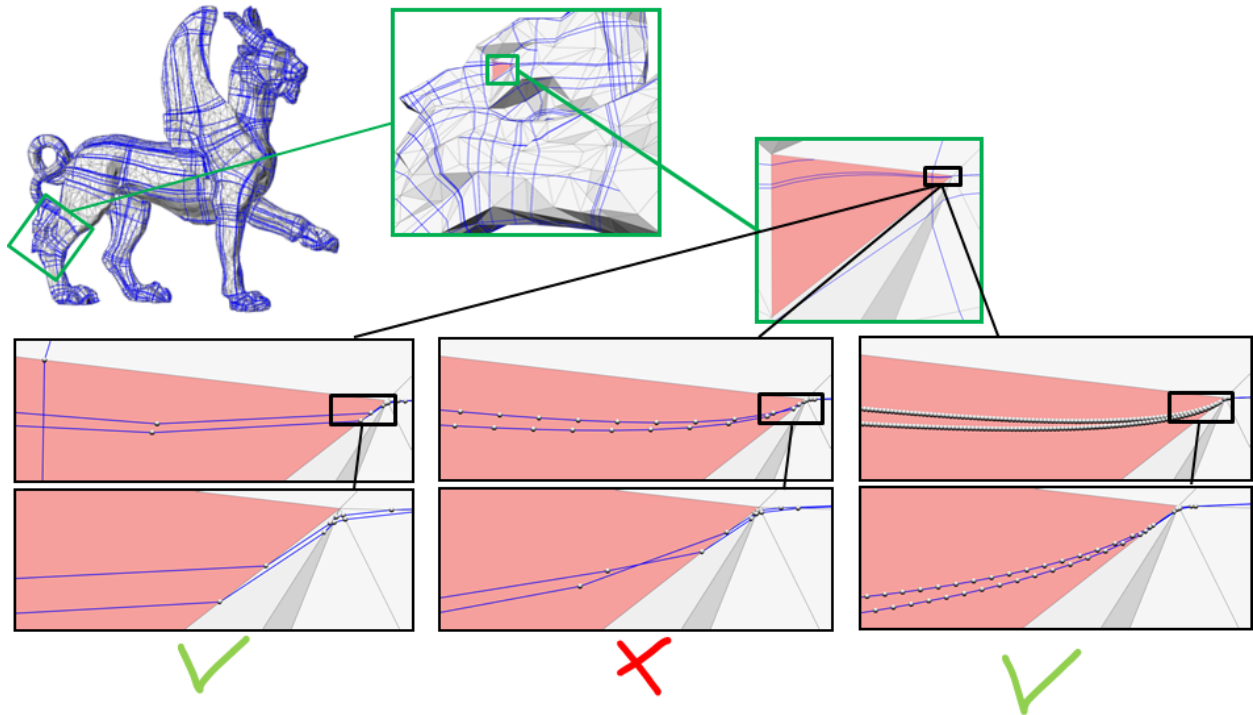


Figure 3: **Numerical integration issues.** Streamlines are traced on a direction field using an order 4 Runge-Kutta with integration step length of (from left to right) $1/10$, $1/100$ and $1/1000$ times the average edge length. A crossing appeared on the pink triangle with $1/10$ and $1/100$ step length.

Algorithm 1: Algorithm overview

Output: Polyline PL
Input: PL extremity halfedge e
Input: PL extremity position c on e
while $e.has_facet()$ AND $c \in [0 \dots 1]$ **do**
 $sm \leftarrow stream_mesh(e.facet())$ (Section 3);
 $e_{sm}, c_{sm} \leftarrow sm.import_position(e, c)$;
 while $e_{sm}.has_facet()$ **do**
 $e_{sm}, c_{sm} \leftarrow$
 $cross_facet(e_{sm}, c_{sm})$ (Section 4);
 end
 $e, c \leftarrow sm.export_position(e_{sm}, c_{sm})$;
 $PL.add_vertex(position(e, c))$;
end

overview of the tangent vector field and, more generally, N-symmetry direction field design algorithms.

Streamline tracing

Tracing streamlines of $2D$ or $3D$ vector fields is a common task [SLCZ09, RT12] in visualization. In most cases, an order four Runge Kutta (RK4) integration scheme performs well. For piecewise linear vector field on a triangulation, a more robust solution [BJB⁺11] was proposed: an edge map directly matches in/out flow intervals of the triangle border. However, they assume the field is defined on vertices and linearly interpolated inside each triangle, and therefore cannot address the vertex angle defect issue (discussed in Section 2).

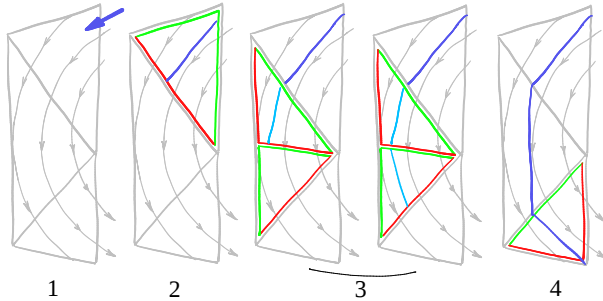


Figure 4: At each step, the algorithm crosses a triangle: a stream-mesh is constructed (green and red halfedges), and the polyline (blue) crosses the stream-mesh. In step 3, the polyline crosses two stream-faces, but the result is a single segment crossing the triangle (visible in step 4).

Tracing curves on triangulated surfaces

Tracing curves on triangulated surfaces is a challenging task because the curve may cross triangles, follow edges, and pass through vertices [LLP05]. All such configurations are naturally managed by our representation: a polyline passing through a vertex is considered as crossing a subset of its adjacent triangles, with all vertices of the polyline located on the vertex of the surface.

For computing optimal systems of loops [CdVL05], one needs to distinguish the order between curves following the same edge, leading to a complex data structure where all curves following the same edge need to be ordered. Special efforts [MVC05,SSK⁺05,PS06] have also been devoted to tracing geodesics where, as in our case, the angle defect plays an important role.

Recent works [SZ12] compute Morse decomposition of piecewise constant vector fields by converting them into a combinatorial structure. It results in a robust algorithm, but the streamlines (edges of the Morse complex) merges due to the input field.

Direction field design

Many algorithms [ZMT06, WWT⁺06, FSDH07] allow to design tangent vector fields. The produced

field can be continuous enough to have (continuous) streamlines that does not cross each others [ZMT06], eventually at the expense of simultaneously refining the surface [WWT⁺06].

For mesh segmentation, it is more common to use N-symmetry direction fields than tangent vector fields but, as pointed by [KNP07]: an N-symmetry direction field is equivalent to a vector field on an N-covering of the surface. Such fields were used for quad remeshing based on global parameterization [RLL⁺06]. The lack of control over these direction fields topology was addressed later [PZ07, RVLL08]. A common representation [RVLL08, RVAL09, BZK09, KNP07] samples the direction on triangles, and explicits the field rotation between adjacent triangles.

2 Field representation

In many cases, it is impossible to trace cross-free streamlines due to the N-symmetry direction field representation. We detail this issue and introduce an alternative representation.

Most representations of tangent vector fields are polynomial on each triangle. These vector fields are differentiable everywhere on each triangle, so their direction expressed as an angle in a local basis of the triangle is also differentiable everywhere except where the vector field is null.

This continuity of the field on triangles also involves discontinuities of the field direction on edges in the vicinity of vertices with non zero angle defect. Indeed, along an infinitesimal circle around the vertex, a unit regular vector field will undergo a rotation that is equal to the vertex angle defect. As the field is differentiable on triangles, the direction rotation accumulated along the cycle necessarily comes from direction discontinuities when crossing edges (Figure 2(b)). Such discontinuities can lead to the merging of streamlines on an edge where the flow outputs both adjacent triangles as in Figure 2(a).

These issues were already addressed in [ZMT06], where they define the field is defined on each vertex by a $2D$ vector in a local map, and interpolated on each triangle. In our case, we want to define a mapping from polyline entry point to polyline out-

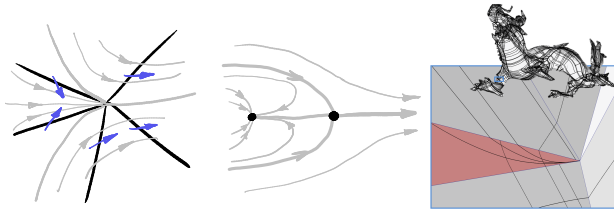


Figure 5: When the field rotation is not homogeneous around a vertex, complex configurations can be represented: the vertex acts as a sink on the leftmost triangle, but as a regular vertex for other triangles (left). The continuous equivalent (middle) is a sink and a saddle, but located on a single vertex. An example is given on the right front leg of the dragon (right).

put point without numerical integration, making it useful to interpolate the field only along edge (not inside triangles). Moreover, we prefer interpolate the field in polar coordinates instead of Cartesian coordinates. It allows to represent more complex fields (with rotation greater than π along an edge), and to better control field singularities by explicitly placing them on vertices.

We represent the input vector field on each triangle by sampling the field direction at each edge extremity: $\alpha_k, k \in [0 \dots 5]$ are the angles of the field, with respect to a reference vector \vec{r} taken in the triangle plane. Note that due to angle defect and singularities on vertex, each vertex is associated to two angles: one for each incident edge.

To prevent crossings, the input field must be continuous across edges i.e have the same angle with respect to an edge on both adjacent triangles of this edge. Another constraint we enforce is to evenly distribute, around each vertex, the angle discontinuity on triangle corners. This later constraint allows to prevent degeneracy (Figure 5) and to better manage singularities (Appendix A.3).

3 Stream-mesh

A stream-mesh is the combinatorial representation of the field behavior inside a triangle of the mesh. It is

a halfedge data structure decorated with additional information that represents the field. The field direction is given at each stream-vertex by its angle α relative to the triangle reference vector \vec{r} . Along each stream-halfedge e , the field have a unique behavior that may be :

- incoming (I) if the field points inwards the stream-face,
- outgoing (O) if the field points outwards the stream-face,
- tangent in the forward direction (T_f) if the field has the stream-halfedge direction,
- or tangent in the backward direction (T_b) if the field direction is opposite to the stream-halfedge direction.

In this representation, we can define:

- An **in-list** as a list of stream-halfedges that contains at least one incoming stream-halfedge, and no outgoing stream-halfedge.
- An **out-list** as a list of stream-halfedges that contains at least one outgoing stream-halfedge, and no incoming stream-halfedge.
- A **simple stream-face** as a stream-face having a border that can be decomposed into an in-list, followed by a forward tangent stream-halfedge, followed by an out-list, and followed by a backward tangent stream-halfedge (Figure 7–right).

The stream-mesh is initialized as a single stream-face by decomposing the triangle border according to the field behavior (Section 3.1). The main stream-face is then decomposed into simple stream-faces by a strategy inspired from the ear clipping algorithm [Ebe98]: simple stream-faces are iteratively removed from the main stream-face until the main stream-face becomes simple (Section 3.2).

3.1 Main stream-face initialization

The initialization of the main stream-face from a triangle is performed independently on each interval

between pairs of field samples. Each interval corresponds either to a triangle edge, or to a corner of the triangle between edge and next edge around the triangle.

For the k^{th} edge E_k of the triangle, the angle of the field with respect to the edge is given by a linear interpolation between $\alpha_{2k} - \angle(\vec{r}, \vec{E}_k)$ and $\alpha_{2k+1} - \angle(\vec{r}, \vec{E}_k)$. When this angle is equal to $0 \bmod 2\pi$ it is a forward tangent, when it is equal to $\pi \bmod 2\pi$ it is a backward tangent, when it is strictly between 0 and $\pi \bmod 2\pi$, it is incoming, and outgoing otherwise. A stream-halfedge is generated for every interval with constant type of behavior, including zero length intervals when the field is tangent at a single point. As illustrated in the second and third columns of the top of Figure 6, tangents are required to characterize the field behavior.

On the triangle corner between k^{th} edge E_k and j^{th} edge E_j (with $j - k = 1 \bmod 3$), α_{2k+1} and α_{2j} may be different due to vertex angle defect or field singularities. As a consequence, it is possible for a vertex to contain important topologic information about the field. As illustrates Figure 6, the field behavior on a vertex (second row) is similar to its behavior along an edge (first row), and can be characterized in the same way. The segmentation is performed with the algorithm described for edges, but angles are linearly interpolated between $\alpha_{2k+1} - \angle(\vec{r}, \vec{E}_k)$ and $\alpha_{2j} - (\angle(\vec{r}, \vec{E}_k) + \angle(\vec{E}_k, \vec{E}_j))$. One can notice that using $\angle(\vec{r}, \vec{E}_k) + \angle(\vec{E}_k, \vec{E}_j)$ instead of $\angle(\vec{r}, \vec{E}_j)$ allows to consider that the triangle border rotation on the corner is in $]0, \pi[$ (not modulo 2π).

A possible geometric interpretation of stream-halfedges generated on triangle corners could be to consider the triangle as a rounded triangle having its corner radius tending to 0. It makes the field and the triangle border rotating along the arc of circle instead of a single point.

3.2 Split the stream-mesh into simple stream-faces

The stream-mesh is now initialized by a main stream-face. The decomposition iteratively removes a simple stream-face from the main stream-face until the main

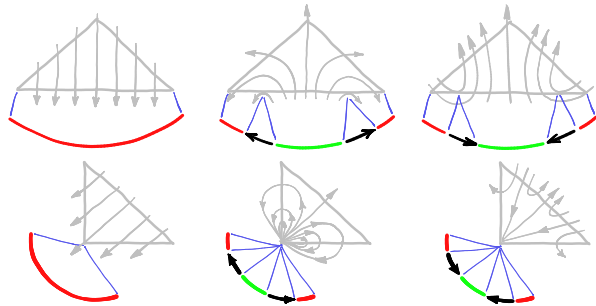


Figure 6: Combinatorial representation of the flow behavior. The first row shows the decomposition of an edge into incoming (green), outgoing (red), tangent forward and backward (black arrows), for three different fields. The second row shows that similar situations can occur on a triangle corner and can be characterized the same way. The field behavior is the same on both rows, but in the second row, the field rotation is performed on a single point instead of a triangle edge. The only difference between columns 2 and 3 is the tangent direction.

stream-face becomes simple (Figure 7).

To remove a simple stream-face (Figure 8), we search in the stream-halfedges list of the main stream-face a sequence of edges that can be decomposed into : a T_f stream-halfedge, followed by an out-list, followed by a T_b stream-halfedge, followed by an in-list, and followed by a T_b stream-halfedge. We split the first T_f and last T_b stream-halfedges of the sequence and introduce a new stream-edge linking the stream-vertices produced by the stream-edge split. The type of produced stream-halfedges is set to incoming in the simple stream-face side, and outgoing in the main stream-face side.

As illustrated by Figure 8, the type of produced stream-halfedges is coherent with the flux that can be computed across the stream-halfedge. Indeed, the triangle border being convex, the field direction at the new stream-halfedge extremities will always point to the same half-plane of the new stream-halfedge. Moreover, the removed sequence prevents high rotations of the field on the stream-halfedge that would make it pointing in the other half-plane inside the

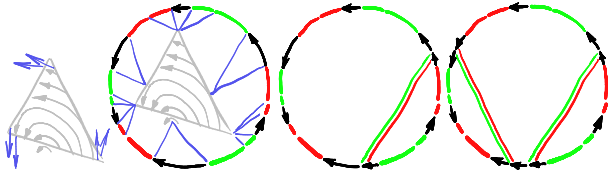


Figure 7: The field is converted into a stream-mesh, then a simple stream-face is removed at each step until the main stream-face become simple.



Figure 8: Splitting the main stream-face (left) by our rule produces a simple stream-face and removes a pair of in-list/out-list of the main stream-face border.

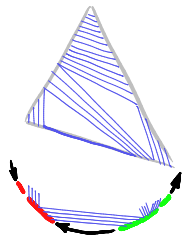
stream-halfedge.

By symmetry, it is also possible to apply the same operation on the opposite field i.e. replace both $T_f \leftrightarrow T_b$ and in-list \leftrightarrow out-list in the pattern and in the result.

Recursively applying the split operation converges to a decomposition into simple stream-faces, as demonstrated in Appendix B.1.

4 Streamline tracing algorithm

Streamlines are traced by iteratively traversing each triangle until it reaches a sink vertex or the surface boundary. Each triangle is traversed by iteratively traversing each simple stream-face (Figure 4) by the algorithm detailed in this section. As illustrated by the inset figure, having polyline's segment inside each triangle results in: some triangular regions of the triangle that are not covered by polylines, and possible local geometric overlaps (on bottom edge). If polylines are dedicated to segment the mesh, such overlaps will re-



sult in faces with degenerated geometry, but it does not affect the combinatorics of the segmented mesh.

4.1 Crossing a simple stream-face

Crossing a simple stream-face requires defining how points of the in-list are mapped to points of the out-list. Any such mapping that does not cross streamlines will produce globally cross-free streamlines. However, it is better to choose a mapping that preserves as much as possible the field geometry. Our mapping is defined such that if an evenly distributed set of streamlines enters the triangle, it will leave it with an even distribution, except if field sinks or streamlines that are tangent to the boundary prevents it. It can be restated as follows: for a normalized field, if the stream-face is split by a streamline, both parts should have the same ratio between inflow and outflow. Here, we call by flux the amount of streamlines outgoing from a portion of the out-list (and symmetrically for the in-list). However, it can be considered as an abuse of terminology since an infinite set of streamlines may leave the triangle in a sink vertex, where the flux should be null. This heuristic perfectly respects the field when it is constant inside the triangle, and is evaluated in Section 5.1 in more difficult situations.

As illustrated in Figure 9, we call f (resp. b) the stream-halfedge of type T_f (resp. T_b) that comes after the out-list (resp. before the in-list).

We denote by $\Phi(e, c)$ the flux crossing the in-list (resp.out) of stream-halfedges up to the point located at the $(c, 1 - c)$ barycentric coordinate on the stream-halfedge e . It is recursively defined by $\Phi(e, c) = \Phi(\text{prev}(e), 1) + \phi_e(c)$ where $\Phi(f, 1) = 0, \Phi(b, 1) = 0$, and $\phi_e(c)$ is the flux crossing the stream-halfedge e up to the point of barycentric coordinates $c, 1 - c$. Computing $\phi_e(c)$ and its inverse are detailed in sections 4.2 and 4.3.

Using these notations (Figure 9), the condition for a streamline to split the simple stream-face into two stream-faces having the same ratio between inflow and outflow writes:

$$\frac{\Phi(e_{in}, c_{in})}{\Phi(\text{prev}(f), 1)} = 1 - \frac{\Phi(e_{out}, c_{out})}{\Phi(\text{prev}(b), 1)}$$

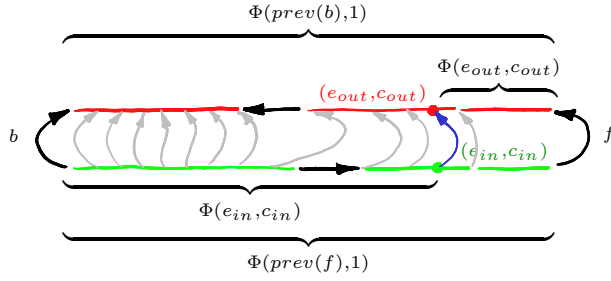


Figure 9: Important flows used to cross a simple stream-face.

where the input point is e_{in}, c_{in} and the output point is e_{out}, c_{out} . As a consequence, the output point is given by :

$$(e_{out}, c_{out}) = \Phi^{-1} \left(\Phi(prev(b), 1) \left(1 - \frac{\Phi(e_{in}, c_{in})}{\Phi(prev(f), 1)} \right) \right)$$

To compute the output position (e_{out}, c_{out}) of a streamline, we need to evaluate the functions Φ , and Φ^{-1} . The function Φ can be evaluated from $\phi_e(c)$ using its recursive definition. The function $\Phi^{-1}(x)$ requires to take the stream-halfedge e such that $\Phi(e, 0) \leq x \leq \Phi(e, 1)$ and $\phi_e(1) \neq 0$, and to define its barycentric coordinate $c = \phi_e^{-1}(x - \Phi(e, 0))$.

As a consequence, we only need to be able to evaluate $\phi_e(c)$ and its inverse $\phi_e^{-1}(x)$ to cross a simple stream-face.

4.2 Computing $\phi_e(c)$

On edges, we set $\phi_e(c)$ to be the flux of the normalized vector field across the stream-halfedge e . The flux across the stream-halfedge is:

$$\begin{aligned} \phi_e(c) &= |\vec{e}| \int_0^c -\sin(\alpha_o + t(\alpha_d - \alpha_o) - \angle(\vec{e}, \vec{r})) dt \\ &= |\vec{e}| \left| \frac{\cos(\alpha_o + t(\alpha_d - \alpha_o) - \angle(\vec{e}, \vec{r}))}{\alpha_d - \alpha_o} \right|_0^c \end{aligned}$$

where α_o and α_d are the field directions located at the vertex pointed by the stream halfedges $prev(e)$ and e , and expressed by their angle relative to \vec{r} .

On corners, we can generally say that there is no flux that leaves the triangle i.e. $\phi_e(c) = 0$. However, for singularities with positive index such as source and sinks, there is an infinity of streamlines that reach or start from the corner (Figure 13). If an out-flow stream-halfedge e is defined in a triangle corner, in a sequence T_f, O, T_b , then we set $\phi_e(c) = c$. By symmetry, if an inflow stream-halfedge e is defined in a triangle corner, in a sequence T_b, I, T_f , then we set $\phi_e = -c$. This strategy provides a field behavior coherent with the continuous behavior of streamlines on field singularities as explained in appendix A.3.

4.3 Computing $\phi_e^{-1}(x)$

Computing $\phi_e^{-1}(x)$ requires to invert Equation (1). As cosine is not a one to one function, determining $\phi_e^{-1}(x)$ requires to take into account that it is a barycentric coordinate in the halfedge e , and therefore $0 \leq \phi_e^{-1}(x) \leq 1$. This constraint fixes $s \in \{-1, 1\}$ and $k \in \mathbb{Z}$ in the formula:

$$\begin{aligned} \phi_e^{-1}(x) &= \frac{s \arccos(\cos(\alpha_o - \angle(\vec{e}, \vec{r}_T)) - x \frac{(\alpha_d - \alpha_o)}{|\vec{e}|})}{\alpha_d - \alpha_o} \\ &+ \frac{2k\pi - \alpha_o + \angle(\vec{e}, \vec{r}_T)}{\alpha_d - \alpha_o} \end{aligned}$$

5 Discussion

This section evaluates the performances and robustness of our algorithm on synthetic stress tests (Section 5.1), proposes some applications where tracing robust streamlines is required (Section 5.2), and provides some implementations details (Section 5.3).

5.1 Synthetic tests

To evaluate the geometric quality of our polylines, we traced them on a circular vector field with different mesh quality (Figure 10). It shows our polylines smoothness and accuracy with different triangle qualities (upper to lower) and different field rotation magnitude (border to center). In practice, computer graphic meshes are closer to the upper and middle

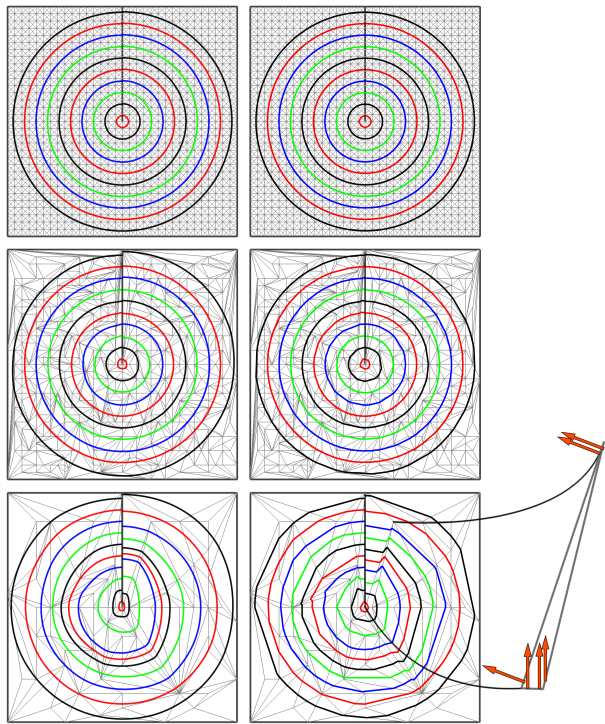


Figure 10: Our algorithm on mesh (right column) is compared with a numerical integration on the same data (left column), with decreasing mesh quality from top to bottom.

images, and field design algorithms tends to produce as smooth as possible fields. It is interesting to notice that an important loss of accuracy only appears (close-up) on very stretched triangles like one having a corner with a field singularity we zoomed on.

The robustness of our algorithm with respect to the mesh geometry is tested in Figure 1(left). No streamlines cross each other, and the loss of quality of the distribution is mostly due to the field smoothing algorithm used to generate the field.

5.2 Applications

We illustrate two possible applications of our method: computing Morse-Smale complexes (Figure 11), and splitting a mesh according to a direction field. Trac-

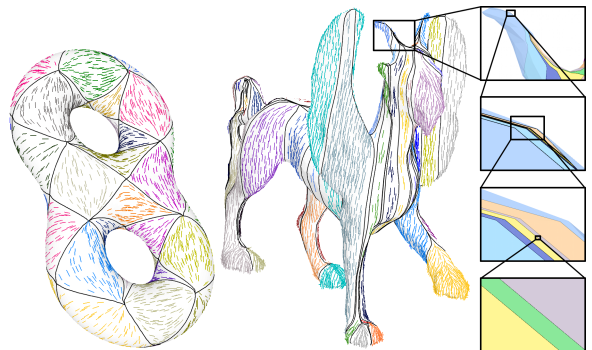


Figure 11: Morse-Smale complexes are computed using a Laplacian eigenfunction for the double torus and the z coordinate for the Feline. Close-ups allow to see that polylines can be very close to each other without merging. The green chart visible in the upper close-up requires an important zoom factor (bottom close-up) to be noticed at the top of the horn.

ing streamlines of a N -symmetry direction field [KLF13] allows to partition $2D$ meshes. To illustrate a possible application of our method, we applied the same strategy on $3D$ surfaces, by growing all streamlines simultaneously, and stopping them when they reach a streamline defined on a perpendicular direction. As a result (Figure 12) we obtain quadrangular charts with T-junctions everywhere except when a degeneracy is prescribed by feature curves as in the fandisk model. Such T-meshes could be useful after optimization, as proposed in [MPKZ10].

5.3 Implementation notes

In our implementation, angles are represented by floating points. A direct consequence is that the border mapping function is one to one only up to numerical precision. More importantly, it could also produce inconsistencies along an edge if its decomposition into stream-halfedges does not match on both adjacent triangles. To prevent streamlines to be stuck inside an edge due to this issue, we always apply the decomposition on the same halfedge, and revert it to obtain the decomposition of the opposite halfedge.

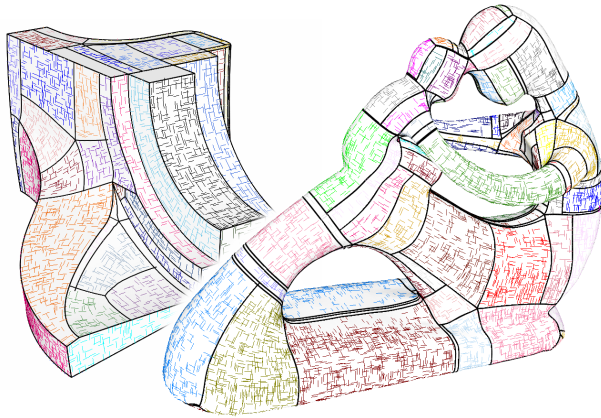


Figure 12: Tracing streamlines (black curves) from singularities of a cross field provides a decomposition of the surface

Another issue comes from applications where the field have to be tangent to an edge. Using the proposed representation, it requires to have $\alpha_{2k} = \angle(\vec{E}_k, \vec{r}') \bmod \pi$ which is usually impossible due to floating point representation. To overcome this difficulty, we represent angles α_{2k} and α_{2k+1} relative to the \vec{E}_k instead of \vec{r}' , and express it in degree (in $[0 \dots 360]$) instead of radian (in $[0 \dots 2\pi]$). Tangents fields are then defined by angles $0 \bmod 180$ which can be exactly represented by floating points.

Conclusion

Tracing intersection-free polylines makes it easier to design new algorithms inspired from the continuous settings. Possible improvements of the method include using polycurves inside triangles, or finding a simpler way to cross each triangle. The question of the generalization to higher dimension arises naturally, but it is important to remember that the main issue (angle defect) requires that the metric is not induced by the object itself (for surfaces, it is induced by its embedding in 3D space, but volumes in 3D do not have this issue).

References

- [ACSD⁺03] Pierre Alliez, David Cohen-Steiner, Olivier Devillers, Bruno Lévy, and Mathieu Desbrun. Anisotropic polygonal remeshing. *ACM Trans. Graph.*, 22(3):485–493, 2003.
- [BJB⁺11] Harsh Bhatia, Shreeraj Jadhav, Peer-Timo Bremer, Guoning Chen, Joshua A. Levine, Luis Gustavo Nonato, and Valerio Pascucci. Edge maps: Representing flow with bounded error. In *Pacific Vis.*, pages 75–82. IEEE, 2011.
- [BZK09] David Bommes, Henrik Zimmer, and Leif Kobbelt. Mixed-integer quadrangulation. *ACM Trans. Graph.*, 28(3):77:1–77:10, 2009.
- [CdVL05] Éric Colin de Verdière and Francis Lazarus. Optimal system of loops on an orientable surface. *Discrete & Computational Geometry*, 33(3):507–534, March 2005.
- [DBG⁺06] Shen Dong, Peer-Timo Bremer, Michael Garland, Valerio Pascucci, and John C. Hart. Spectral surface quadrangulation. *ACM Trans. Graph.*, 25(3):1057–1066, 2006.
- [Ebe98] David Eberly. Triangulation by ear clipping. *Geometric Tools*, 1998.
- [FSDH07] Matthew Fisher, Peter Schröder, Mathieu Desbrun, and Hugues Hoppe. Design of tangent vector fields. *ACM Trans. Graph.*, 26:56, 2007.
- [KLF13] Nicolas Kowalski, Franck Ledoux, and Pascal Frey. A pde based approach to multidomain partitioning and quadrilateral meshing. In *Proceedings of the 21st International Meshing Roundtable*, pages 137–154. Springer Berlin Heidelberg, 2013.

- [KNP07] Felix Kälberer, Matthias Nieser, and Konrad Polthier. Quadcover - surface parameterization using branched coverings. *Comput. Graph. Forum*, 26(3):375–384, 2007.
- [LLP05] Wan Chiu Li, Bruno Lévy, and Jean-Claude Paul. Mesh editing with an embedded network of curves. In *IEEE International Conference on Shape Modeling and Applications*, pages 62–71, 2005.
- [MI95] Marian Mrozek and Instytut Informatyki. Conley index theory. In *Handbook of Dynamical Systems II, North-Holland*, pages 393–460. Elsevier, 1995.
- [MPKZ10] Ashish Myles, Nico Pietroni, Denis Kovacs, and Denis Zorin. Feature-aligned t-meshes. In *ACM SIGGRAPH 2010*, pages 117:1–117:11, 2010.
- [MVC05] Dimas Martínez, Luiz Velho, and Paulo C. Carvalho. Computing geodesics on triangular meshes. *Comput. Graph.*, 29(5):667–675, October 2005.
- [PS06] Konrad Polthier and Markus Schmies. Straightest geodesics on polyhedral surfaces. In *ACM SIGGRAPH 2006 Courses, SIGGRAPH '06*, pages 30–38, New York, NY, USA, 2006. ACM.
- [PZ07] Jonathan Palacios and Eugene Zhang. Rotational symmetry field design on surfaces. *ACM Trans. Graph.*, 26(3):55, 2007.
- [RLL⁺06] Nicolas Ray, Wan Chiu Li, Bruno Lévy, Alla Sheffer, and Pierre Alliez. Periodic global parameterization. *ACM Trans. Graph.*, 25(4):1460–1485, October 2006.
- [RT12] C. Rossel and H. Theisel. Streamline embedding for 3d vector field exploration. *IEEE Transactions on Visualization and Computer Graphics*, 18(3):407–420, march 2012.
- [RVAL09] Nicolas Ray, Bruno Vallet, Laurent Alonso, and Bruno Lévy. Geometry aware direction field processing. *ACM Transactions on Graphics*, pages 1:1–1:11, 2009.
- [RVLL08] Nicolas Ray, Bruno Vallet, Wan Chiu Li, and Bruno Lévy. N-symmetry direction field design. *ACM Trans. Graph.*, 27(2):10:1–10:13, May 2008.
- [SLCZ09] Benjamin Spencer, Robert S. Laramee, Guoning Chen, and Eugene Zhang. Evenly spaced streamlines for surfaces: An image-based approach. *Comput. Graph. Forum*, 28(6):1618–1631, 2009.
- [SSK⁺05] Vitaly Surazhsky, Tatiana Surazhsky, Danil Kirsanov, Steven J. Gortler, and Hugues Hoppe. Fast exact and approximate geodesics on meshes. *ACM Trans. Graph.*, 24(3):553–560, July 2005.
- [SZ12] Andrzej Szymczak and Eugene Zhang. Robust morse decompositions of piecewise constant vector fields. *IEEE Transactions on Visualization and Computer Graphics*, 18:938–951, 2012.
- [WWT⁺06] Ke Wang, Weiwei, Yiying Tong, Mathieu Desbrun, and Peter Schröder. Edge subdivision schemes and the construction of smooth vector fields. *ACM Trans. Graph.*, 25(3):1041–1048, July 2006.
- [ZMT06] Eugene Zhang, Konstantin Mischaikow, and Greg Turk. Vector field design on surfaces. *ACM Trans. Graph.*, 25(4):1294–1326, October 2006.

A Behavior on vertices

A.1 Vertex indices

N-symmetry direction fields may have singularities that can be characterized by their index. The index is well defined for smooth manifolds [MI95], and has been extended to triangulated surfaces [RVAL09]. In

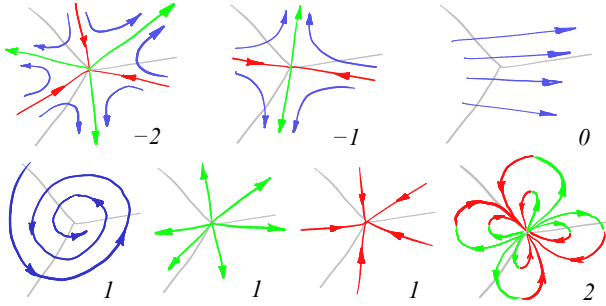


Figure 13: Singularities classified by index. On negative indices, there exist a finite number of streamlines (red and green) having the vertex as extremity. On regular vertices (index is zero), at most one streamline can cross the vertex. On positive index singularities, there exist an infinity of streamlines having the vertex as extremity, except for the vortex case (lower-left).

our case, we assume that singularities can only appear on vertices, leading to the following characterization of indices:

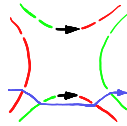
$$Index(A) = \sum \frac{\Delta\alpha_e}{2\pi} + \frac{2\pi - \sum \beta_e}{2\pi} \quad (1)$$

where the sums are performed on all triangle corners referred by their halfedge e incident to A , $Index(A)$ is the index of vertex A , $\Delta\alpha_e$ is the angle discontinuity on the triangle corner, β_e is the triangle corner angle. The first sum is the total amount of field rotation around A , and the rest is the angle defect of A divided by 2π .

Examples of singular vertices are given in Figure 13. One can notice that an infinite number of streamlines can reach the vertex only for strictly positive indices, leading to two different behaviors of our algorithm as detailed below.

A.2 Geometric vertex crossing

The default behavior of our algorithm is when there is not an infinity of streamlines having the vertex as one of its extremities. In this case, when a streamline leaves a triangle on a vertex location, the



output of the triangle crossing algorithm is an adjacent edge, with a barycentric coordinate being either 0 or 1 to fit the vertex location. The streamline then continues on the next triangle until it ends in the vertex or leaves the vertex location as illustrated in the small figure to the right.

Our algorithm has this behavior because the flux on a stream-halfedge defined on a triangle corner is generally zero, and the constraint that the simple stream-face crossing algorithm is not allowed to generate outputs on a stream-halfedge without flux.

A.3 Streamline extremity on a vertex

Streamlines may also have one of its extremities located on a vertex, but this occurs only for vertices with strictly positive index, as illustrated in Figure 13 (we consider that if a unique streamline reach the vertex it will cross it with the previous behavior). We explain here why our way to determine the flux on stream-halfedges inside triangle corners (Section 4.2) gives non zero flux only for vertices with strictly positive index.

As the rotation speed of the field around the vertex A is constant, the difference of angle $\Delta\alpha_e$ is equal to the sum of such rotations around the vertex A times the ratio of β_e over the sum of triangle corner angles around A . Putting it together with equation (1), with summation over all halfedges e' pointing to A gives:

$$\Delta\alpha_e = \frac{\beta_e}{\sum \beta_{e'}} \left(2\pi(Index(A) - 1) + \sum \beta_{e'} \right)$$

so the variation of angle with respect to halfedges pointing to A is

$$\Delta\alpha_e - \beta_e = \frac{2\pi\beta_e}{\sum \beta_{e'}} (Index(A) - 1)$$

As a consequence, if $\Delta\alpha_e - \beta_e$ is strictly positive, the vertex index is greater or equal to 1. Else, the index is strictly less than 1. Note that for direction fields with rational indices, we are still able to distinguish between singularities with and without flux.

In our algorithm, the condition to associate some flux to output stream-halfedges (defined on a triangle

corner) is that the stream-halfedge must be contained in a sequence T_fOT_b . It means that the field angle with respect to the triangle border increases at least by π . Since the corner is convex, we have $\beta_e < \pi$. As a consequence, our algorithm gives some flux only for stream-halfedges in triangle corners corresponding to a vertex with strictly positive index. The same thing occurs for the sequence T_bIT_f .

A.4 Starting a streamline from a vertex

For vertices that are the origin of a finite number of streamlines (negative or null index), it is possible to generate all streamlines by simply starting a streamline for each inflow stream-halfedge on adjacent triangle corners. This is especially important for tracing streamlines from saddle points, as it is required for computing Morse-Smale complexes.

B Correctness of the decomposition

B.1 Convergence

Given a stream-face with n in-lists and n out-lists, let us choose one out-list as a reference. Any two adjacent lists i and $i + 1$ have a tangent between them, let us define a sequence of labels $\{t_i\}_{i=0}^{\infty}$ as the label of tangent stream-halfedge incident to both lists i and $i + 1$. Then we define a sequence of integers $\{a_i\}_{i=0}^{+\infty}$ as follows:

$$\begin{aligned} a_0 &= 0 \\ a_{2i+1} &= \begin{cases} a_{2i} + 1 & \text{if } t_{2i+1} = T_f, \\ a_{2i} - 1 & \text{otherwise.} \end{cases} \\ a_{2i+2} &= \begin{cases} a_{2i+1} + 1 & \text{if } t_{2i+2} = T_b, \\ a_{2i+1} - 1 & \text{otherwise.} \end{cases} \end{aligned}$$

The defined sequence $\{a_i\}$ is arithmetic quasiperiodic: $a_{i+2n} = a_i - 2$ and is continuous in the sense that $|a_{i+1} - a_i| = 1$. A stream-face is simple if and only if the corresponding sequence $\{a_i\}$ is decreasing. The splitting rule described in section 3.2 searches

for a pattern (per period $2n$) $(2i + 1, 2i, 2i - 1, 2i)$ in the sequence $\{a_i\}$ and replaces it with a new one $(2i + 1, 2i)$. In other words, the splitting rule removes one (per period) local minimum of the sequence $\{a_i\}$. The symmetric rule replaces $(2i + 2, 2i + 1, 2i, 2i + 1)$ with $(2i + 2, 2i + 1)$, again removing a local minimum. If a stream face is not simple, the corresponding sequence has at least one local minima, moreover, the sequence decreases by 2 with each period and therefore it is possible to apply one of the splitting rules. Both rules keep the continuity of the sequence, and the period is reduced by 2 with each iteration, leading to a final decomposition of the initial stream-face into a set of simple stream-faces.

B.2 Non-nullity of flux through simple faces

We show that each simple stream-face is traversed by some flux. To do so we demonstrate that the out-list (as well as in-list) of a simple stream-face have non-zero associated flux.

First of all, let us note that all stream-halfedges created by splitting rules have non-zero flux. Indeed, their length is not zero: it is easy to see that due to the linear interpolation between angle samples, the sequence $\{a_i\}$ is monotonic inside triangle corners; however the splitting rule searches for a local minimum of the sequence. Therefore, it is not possible to create a simple face entirely contained in a triangle corner.

Now let us show that all simple faces have non-zero flux through them. Let us suppose that the out-list of a simple stream-face has a zero flux. All outflow stream-halfedges on triangle edges as well as outflow stream-halfedges corresponding to splits have non-zero flux, since their length is greater than zero. The only option for an out-list to have a zero flux is to be contained in a triangle corner and to have T_b, O, T_f structure, as defined in section 4.2. However it means that the corresponding sequence $\{a_i\}$ is increasing on this out-list, and that contradicts the monotonicity of the sequence $\{a_i\}$ for simple faces. Therefore, there is no out-list in a simple face that does not have a flux through it. The same argument shows by symmetry that there is no in-list without flux through it.